U. S. DEPARTMENT OF COMMERCE
Luther H. Hodges, Secretary
WEATHER BUREAU
F. W. Reichelderfer, Chief

NATIONAL SEVERE STORMS PROJECT

REPORT No. 3

Instability Lines and Their Environments As Shown By Aircraft Soundings and Quasi-Horizontal Traverses

by
Dansy T. Williams
National Severe Storms Project, Kansas City, Mo.

Washington, D. C.
February 1962

CONTENTS

		Page
1.	INTRODUCTION	1
2.	DATA ADJUSTMENTS	1
3.	AVERAGE SOUNDINGS OF INSTABILITY LINE ENVIRONMENTS	2
4.	SPACE CROSS SECTIONS OF INSTABILITY LINE ENVIRONMENTS	4
5.	AVERAGE CROSS SECTIONS OF INSTABILITY LINE ENVIRONMENTS	5
6.	THE CASES OF MAY 16, 1960, AND MARCH 25, 1959	7
7.	THE ADDITION OF DETAIL FROM TRAVERSES	9
8.	ISENTROPIC GEOMETRY AND MOTION FIELDS	11
9.	SUMMARY	14
	REFERENCES	15

INSTABILITY LINES AND THEIR ENVIRONMENTS AS SHOWN BY AIRCRAFT SOUNDINGS AND QUASI-HORIZONTAL TRAVERSES*

Dansy T. Williams
National Severe Storms Project
Kansas City, Mo.

1. INTRODUCTION

During the 1958-1960 operation of the Weather Bureau instrumented P-38 Research Airplane [1], the taking of soundings was an important part of its observational program. Soundings consisted of temperature, humidity, and pressure-altitude, and were made ideally as spiral ascents or descents at 1,000 ft./min. between 850 and 500 mb. Many were made in the vicinity of instability lines. The aircraft also made horizontal and quasi-horizontal traverses across instability lines. Traverses at constant pressure levels have already been studied by Lee and David [1].

It is the purpose of this paper to present some features of the instability line and its environment, as shown by selected pairs of the aircraft soundings. Space cross sections, using both sounding and quasi-horizontal traverse data, are also shown and are used as a basis for a qualitative model of the motion fields in the instability line and its environment.

Sounding pairs were selected that met the following requirements: (1) Observations made in sufficient depth to be worthwhile (usually 850 to 500 mb.), (2) Soundings an adequate distance apart (spacing ranged from 80 to 165 statute mi. with an average spacing of 112 mi.), (3) Time interval between soundings sufficiently short to permit synoptic analysis (time intervals ranged from 25 to 94 min. with an average interval of 54 min.), and (4) Individual observations on both sides of, but not inside the instability line. Nineteen sounding pairs were found that met these requirements.

2. DATA ADJUSTMENTS

In a few cases soundings did not extend quite down to the 850-mb. level. In these cases surface values of temperature and dew point were used to provide interpolated values for the missing levels.

Values of potential temperature were obtained by reading off the values from the plots of temperature on pseudo-adiabatic charts.

---

* Presented in part at the Conference on Severe Storms, St. Louis, Mo., May 11, 1960

Moisture data were in the form of mixing ratio. Relative humidity values were obtained when needed from pseudo-adiabatic charts by forming the ratio between aircraft values of mixing ratio and the saturation values for the temperatures and pressure-altitudes of individual points.

Previous work of Lee and David [2] was used to locate instability lines with respect to sounding pairs. Manuscript surface charts of the Severe Local Storms Center and radar plots of the Radar Analysis and Development Unit were also used. Individual instability lines were not classified as to type; however, more than half of them were of the pre-cold frontal type.

In computing spatial gradients with respect to moving lines, motions of the lines and their orientations with respect to the sounding pairs were considered. In figure 1 the distance between soundings, AB, was converted to an effective normal distance, N, equal to $AB \cos \phi \pm ct$, where ϕ is the angle between AB and its normal projection to the line, CD; c is the speed of movement of the line (as measured from surface synoptic charts and radar plots); and the t is the time interval between soundings. N is equal to CD' or $CD - ct$, when sounding A is made at t_o and sounding B is made at t_1. N is equal to $C'D$ or $CD + ct$, when sounding B is made at t_o and sounding A is made at t_1.

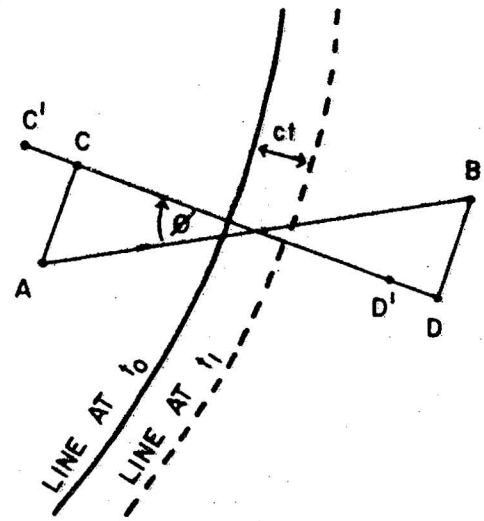

Figure 1. --Adjustment to achieve a time-space equivalence with respect to a moving line.

3. AVERAGE SOUNDINGS OF INSTABILITY LINE ENVIRONMENTS

Sounding pairs were classified according to stage of instability line development, the number of pairs in each category being: Incipient stage — 4, Active stage — 13, and Dissipating stage — 2. Individual soundings were averaged to obtain mean soundings for each of the first two categories.

Incipient stage. These included cases ranging from no clouds at all to cases in the early cumulus stage. The averages undoubtedly suffer from the small number of cases.

The mean sounding ahead of the incipient line (fig. 2) shows conditions at an average effective normal distance 22 mi. in advance of the line. There was considerable moisture below 800 mb., a drier layer centered near 700 mb., and a thermally more stable layer between 800 and 750 mb. The Showalter Stability Index, SI, [3] was -2.5, and the Level of Free Convection, LFC was at 590 mb. for a parcel lifted from 850 mb.

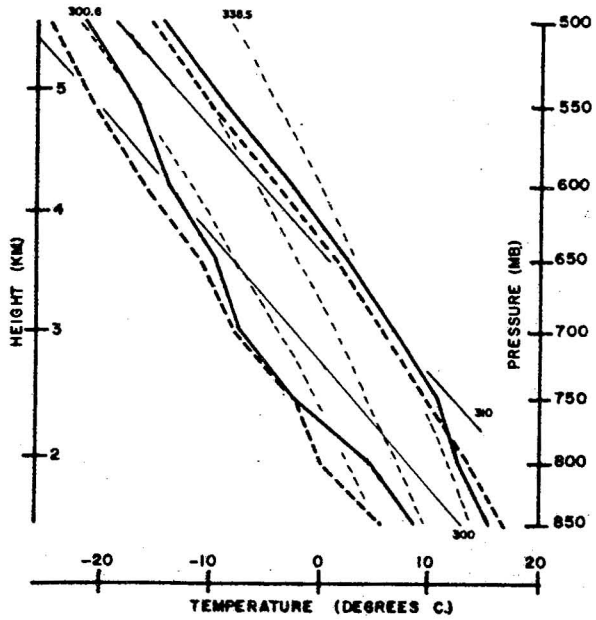

Figure 2.- Average sounding 22 mi. ahead of the leading edge of an incipient instability line (solid plot) and average sounding 95 mi. back of the leading edge of an incipient instability line (dashed plot).

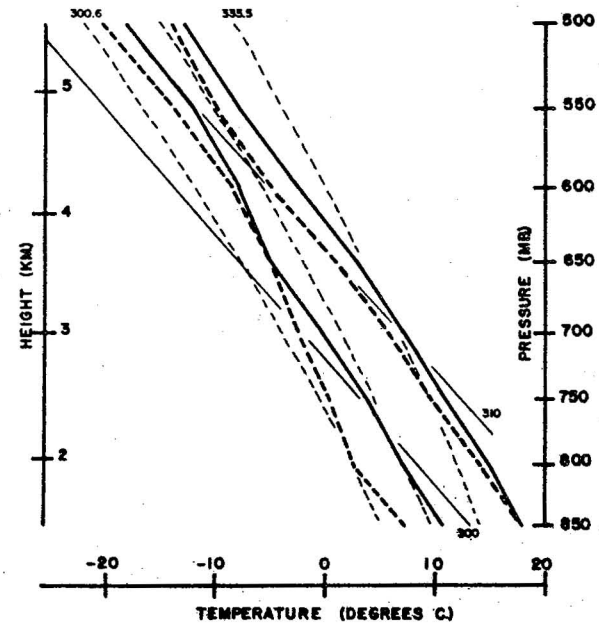

Figure 3.- Average sounding 27 mi. ahead of the leading edge of an active instability line (solid plot) and average sounding 78 mi. back of the leading edge of an active instability line (dashed plot).

The mean sounding behind the incipient line (fig. 2) shows conditions at an average effective normal distance 95 mi. behind the leading edge of the line. (Due to difficulties in determining a unique trailing edge to many of the lines all distances were computed with respect to the leading edge of the line). As compared to the mean sounding ahead of the line, its low level moisture was less, its SI was greater (-1.0), and its LFC was higher (565 mb.). There was no marked layer of greater thermal stability.

Active Stage. These included cases in which active thunderstorms were occurring along the line. The number of cases is probably sufficient, although the lower portions of the mean soundings are somewhat smoothed as the result of using interpolated values in a few of the cases.

The mean sounding ahead of the active line (fig. 3) shows conditions at an average effective normal distance of 27 mi. in advance of the line. The moisture lapse rate was fairly uniform, but with greater relative humidity at lower levels. The temperature lapse rate was also fairly uniform. The SI was -3.5 and the LFC was at 650 mb.

The mean sounding behind the active line (fig. 3) shows conditions at an average effective normal distance 78 mi. behind the leading edge of the line. The moisture lapse rate was fairly uniform but with much greater relative humidity at higher than at lower levels. As compared with the sounding ahead of the line, its low level moisture was considerably less, while its upper level moisture was only slightly less. The temperature lapse rate was nearly dry adiabatic from 650 to 600 mb., but with increasing thermal stability above 600 mb. The SI was greater (-1.5) and the LFC was slightly higher (630 mb.) than was the case ahead of the line.

Dissipating Stage. These included cases in which soundings were made after thunderstorm activity had ceased. Although the number of cases was too few to permit valid averages, the individual soundings were considerably drier at all levels than those of the incipient and active stages, and their stability was greater.

4. SPACE CROSS SECTIONS OF INSTABILITY LINE ENVIRONMENTS

Sounding pairs were used to construct space cross sections of potential temperature and mixing ratio. An example of such a cross section is shown in figure 4. Isopleths have been drawn simply as straight lines between appropriate points on each sounding. They portray the gross environment in which the active instability line was embedded. They do not, of course, show detailed conditions in the instability line itself.

It may be noted in figure 4 that the slope of isentropes is positive (upward from left to right and from behind to in advance of the line) below 2.0 km. and negative (downward from left to right and from behind to in advance of the line) above 2.5 km. Isopleths of mixing ratio, have a marked positive slope at low level, while those above 3.0 km. have very little slope. Spacing of isentropes indicates that with respect to temperature alone the atmosphere was more stable at Snyder than at Hobbs, and that the layer from the surface to 3.5 km. was very nearly dry adiabatic at Hobbs. However, considering both temperature and moisture, the atmosphere was more stable at Hobbs than at Snyder.

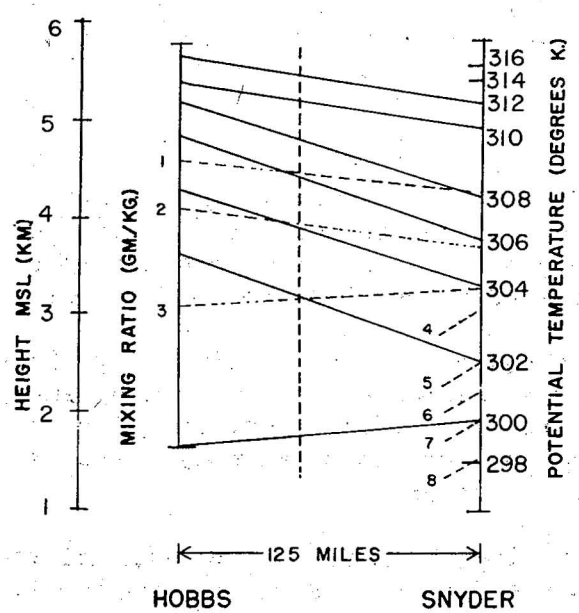

Figure 4.– Space cross section of potential temperature and mixing ratio between Hobbs, New Mexico, and Snyder, Texas, Flight 24, 1608-1701 CST, March 28, 1958. Isentropes are drawn for each 2° K. and mixing ratio isopleths are drawn for each gm./kg. Leading edge of the instability line is shown as a heavy dashed, vertical line.

5. AVERAGE CROSS SECTIONS OF INSTABILITY LINE ENVIRONMENTS

Seventeen cases were used to construct average cross sections of potential temperature and mixing ratio for the incipient and active stages. Distances in the sections are mean effective normal distances between sounding pairs.

Slopes of isentropes were obtained by forming ratios of the height differences of the isentropes at the ends of the sections with respect to the effective normal distances of the sections. As an example, the 302° K. isentrope for the Hobbs to Snyder section in figure 4 had a height difference of 1100 m. along its 125 mi. distance. Since the effective normal distance was 102 mi. or 164 km., the slope would be -1100 m./164 km. or -6.7 m./km. Average slope of isentropes was obtained in the same way from the average cross sections.

Incipient Stage. The average cross section is shown in figure 5, and some of its features are summarized in Table 1. The mean effective normal distance was 117 mi., and the mean distance to the leading edge of the incipient line was 22 mi. Mean isentropes sloped upward slightly at low level, but became increasingly negative in slope with height until a maximum negative slope of -4.8 m./km. was reached at 4.2 km. Individual slopes were negative everywhere from 3 to 5 km. The low level moisture ahead of the line was considerable and it was stratified somewhat. Values ranged from 8 gm./kg. at 1.5 km. to 4 gm/kg. at 2.4 km. The low level moisture behind the line was less with values ranging from 6 gm./kg. at 1.6 km. to 4 gm./kg. at 2.5 km. The mean isopleths of mixing ratio sloped upward at all levels, although the slope at 2.5 km. was nearly zero.

Table 1. Summary of potential temperature features of space cross sections normal to incipient instability lines (4 cases).

Level (km.)	1.5	2.0	3.0	4.0	5.0	5.5
Range of isentropic slope (m./km.)	3.4	1.5	-1.7	-1.3	-0.4	0.0
	-0.2	-1.5	-7.9	-17.1	-16.7	-5.5
Average isentropic slope (m./km.)	2.3	0.5	-2.5	-4.5	-3.8	-3.0
Percent with positive slope	50	50	0	0	0	25
Percent with negative slope	50	50	100	100	100	75

Active Stage. The average cross section is shown in figure 6, and some of its features are summarized in Table 2. The mean effective normal distance was 105 mi., and the mean distance to the leading edge of the active line was 27 mi. The mean isentropes had negative slope at all levels, except for a slight positive slope at 1.5 km. There was maximum negative slope of -6.8 m./km. at the 4.3 -km. level. Individual slopes were negative everywhere from 4 to 5 km. Similar negative slopes of isentropes were indicated in a model by Fulks in 1951 [4]. The low level moisture ahead of the line

was considerable, but the stratification was not so great as in the incipient stage. The values ranged from 9 gm./kg. at 1.5 km. to 4 gm./kg. at 3.5 km. The low level moisture behind the line was less with values ranging from 7 gm./kg. at 1.5 km. to 4 gm./kg. at 3.5 km. Mean isopleths of mixing ratio sloped upward at levels below 3.0 km., but had little or no slope above 3.0 km.

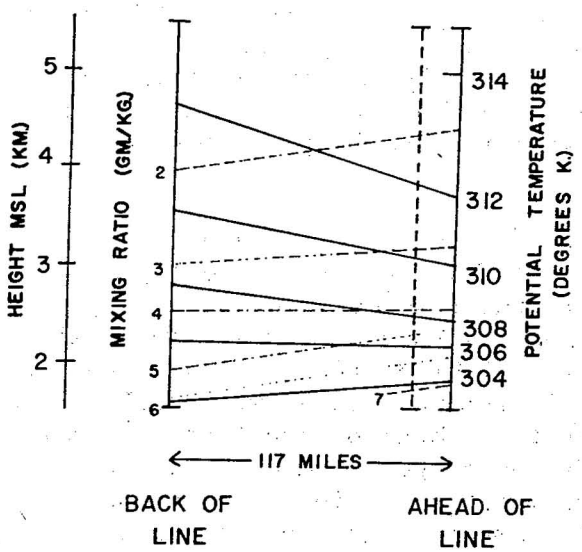

Figure 5.– Average space cross section of the potential temperature and mixing ratio environment for an incipient instability line (average of 4 cases).

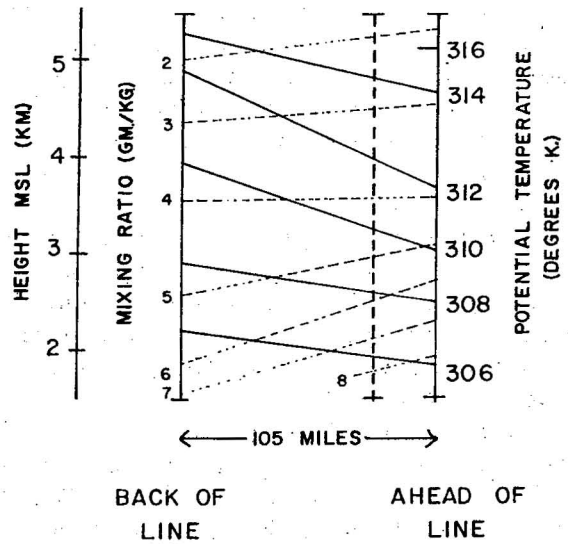

Figure 6.– Average space cross section of the potential temperature and mixing ratio environment for an active instability line (average of 13 cases).

Table 2. Summary of potential temperature features of space cross sections normal to active instability lines (13 cases).

Level (km.)	1.5	2.0	3.0	4.0	5.0	5.5
Range of isentropic slope (m./km.)	6.3	4.2	2.0	-4.1	-1.3	1.3
	-10.5	-20.0	-12.8	-11.3	-12.2	-9.8
Average isentropic slope (m./km.)	0.1	-2.1	-3.5	-6.3	-3.6	-1.8
Percent with positive slope	54	46	15	0	0	23
Percent with negative slope	46	54	85	100	100	77

Dissipating Stage. Cases were too few to permit the construction of a valid mean cross section. In one case isentropes sloped negatively from 2.2 to 4.0 km. In the other case there was slight negative slope at all levels.

6. THE CASES OF MAY 16, 1960, AND MARCH 25, 1959.

These cases were of interest, since they were associated with severe thunderstorm activity, and since the amount of their isentropic slopes was great. Their effective normal distances were quite short (25 and 28 mi. respectively), so they have not been included in the nineteen cases just presented.

The case of May 16, 1960---An incipient case. The instability line which became active around 1600 CST was oriented northeast-southwest through the Oklahoma City vicinity. The line was virtually stationary for the next three hours, and it is assumed that the incipient line had been in the same location for some hours before. The 1200 CST Oklahoma City sounding and an aircraft sounding 35 mi. east of Oklahoma City at 1211 CST provide a short cross section through the incipient line.

The cross section is shown in figure 7. The steep negative slope of the isentropes may be noted. Greatest slope was -104 m./km. at 4.9 km. This is over 25 times the average shown in Table 1 for the 5.0-km. level. In this case the main low level moisture was well below the 1.8-km. level of the cross section base. A dry layer sloped downward from 2.3 km. at Oklahoma City to 1.8 km. at the point east of Oklahoma City, while an intermediate level moist layer sloped downward from 3.2 km. at Oklahoma City to 2.6 km. at the point east of Oklahoma City.

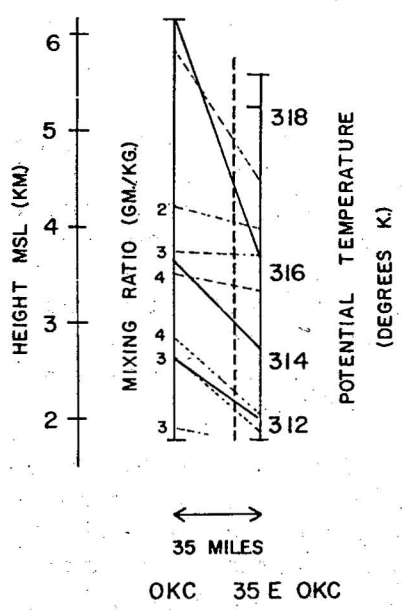

Figure 7.- Space cross section of potential temperature and mixing ratio across a strong, incipient instability line between Oklahoma City, Oklahoma (OKC), and a point 35 mi. east (35 E OKC), Flight 47, 1200-1227 CST, May 16, 1960.

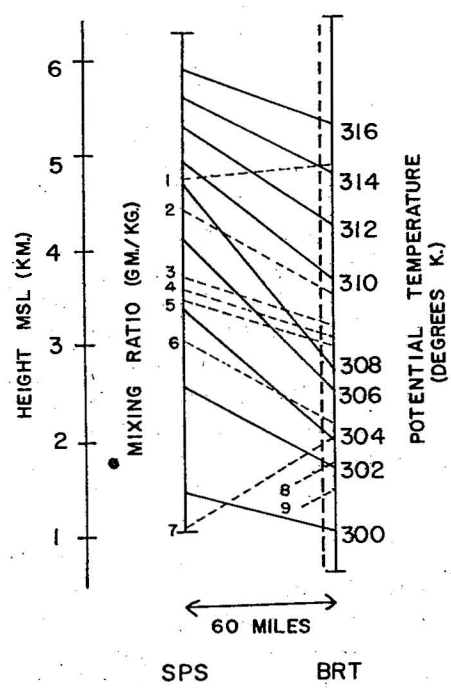

Figure 8.- Space cross section of potential temperature and mixing ratio across a strong, active instability line between Wichita Falls, Texas (SPS), and Bridgeport, Texas (BRT), Flight 10, 1448-1536 CST, March 25, 1959.

The 1200 CST Oklahoma City winds aloft were approximately southwest. The *u*-component of the wind, which is the component parallel to the section in figure 7, had values ranging from 11 to 24 m./sec. through the layer from 2 to 6 km.

Severe weather associated with this instability line included 1½-in. hail at Oklahoma City at 1745 CST and at Chickasha, Oklahoma at 1900 CST. In addition to this, the T-33 aircraft of the National Severe Storms Project encountered softball size hail at the 38,000 - 40,000 feet level 30 miles south of Oklahoma City at 1700 CST.

The case of March 25, 1959--- An active case. The instability line was oriented nearly north-south and was moving eastward through northern Texas. The P-38 aircraft was on the ground at Wichita Falls, Texas, when the line passed. Following passage, the aircraft made an ascent sounding behind the line over Wichita Falls, flew southeastward over the line, and then made a descent sounding just ahead of the line near Bridgeport, Texas. The soundings were made 60 mi. apart, but corrections for the angle at which the line was traversed (40 degrees) and the speed of movement of the line (20 kt.) gave an effective normal distance between soundings of only 28 mi.

The cross section is shown in figure 8. The steep negative slope of the isentropes may again be noted. Greatest slope was -40 m./km. at 3.8 km. This is about six times the average shown in Table 2 for the 4.0-km. level. Low level moisture was greatest ahead of the line, but at intermediate levels it was slightly more behind the line. Some stratification of moisture was apparent---near 2 and 3 km. ahead of the line and near 3.5 km. behind the line. It appears that there had been a net lift of moisture behind the line at intermediate levels, even to the point of maintaining the stratification during lift.

No winds sufficiently close in time and space were available for reference to the section in figure 8. However, the 1200 CST winds aloft at Fort Worth were approximately southwest and normal to the section, with speeds ranging from 5 m./sec. at 1 km. to 24 m./sec. at 6 km. Although the winds were normal to the section itself, they did have a component across the instability line, since the line was oriented approximately north to south.

Severe weather associated with this line included funnel clouds about 30 mi. north of Wichita Falls at 1410 CST and 1430 CST; 1-in. hail at Ardmore, Oklahoma, at 1606 CST; a funnel cloud at Gainesville, Texas, at 1700 CST; and 1½-in. hail at Perrin AFB, Texas at 1801 CST.

In the two cases above, some of the steepness of the isentropic slopes undoubtedly resulted from the shortness of the effective normal distances. In the first case it may have resulted also from the fact that the Oklahoma City sounding was probably within, rather than to the rear of, the incipient line. However, it is also indicated that some of the steepness may have been related to the severity of the storms.

7. THE ADDITION OF DETAIL FROM TRAVERSES

In some cases the two soundings comprising a cross section were connected by a quasi-horizontal traverse. The traverses were made in clear air over, under, or between clouds in the case of active instability lines. In such cases isentropes at the traverse level were adjusted to fit the traverse data, and the geometry of these isentropes was assumed for isentropes immediately above and below the traverse level. The addition of a traverse near 500 mb. to the Hobbs - Snyder section of March 28, 1958 (fig. 4) is shown in figure 9. An upward bulging of isentropes in the vicinity of the instability line may be noted. Three additional traverses are shown in figures 10-12. Moisture values were available for two of these and are shown as relative humidity profiles (smoothed for 2-min. periods) in figures 11 and 12. In each of the cases there was an upward bulging of isentropes immediately behind the leading edge of the instability line. Width of this bulge was sometimes greater than the visual or radar width of the instability line.

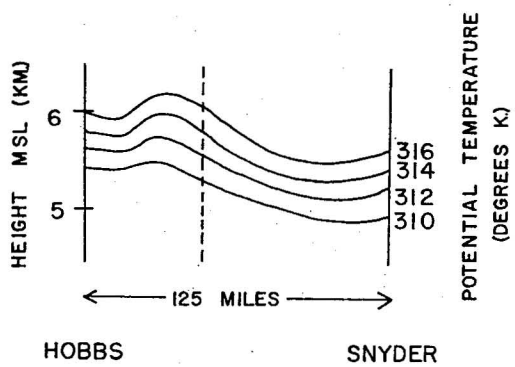

Figure 9.- The addition of isentropic detail from a horizontal traverse near 5.5 km. to the space cross section shown in figure 4.

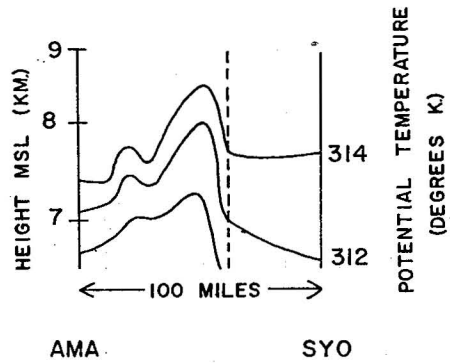

Figure 10.- Isentropic detail from a quasi-horizontal traverse through an active instability line between Amarillo, Texas (AMA), and Sayre, Oklahoma (SYO), Flight 27, 1544-1656 CST, April 2, 1958.

In the Amarillo, Texas, to Sayre, Oklahoma, section (fig. 10) the bulge in isentropes is quite pronounced. A smaller bulge immediately to the rear suggests that a secondary line was also traversed or that there may have been a wave pattern to the isentropes.

In the Wichita Falls, Texas, to McAlester, Oklahoma, section (fig. 11) the gradual bulge in isentropes in the right portion of the section coincided with an incipient area ahead of a surface cold front. It was anticipated that an instability line would form in this area, but possibly due to the great stability of the air mass (the SI was +10), none formed. The relative humidity profile shows that very dry air was present at the traverse level with the driest air over McAlester and air of lesser dryness from the region of the isentropic bulge westward toward Wichita Falls.

In the Abilene, Texas, to Mineral Wells, Texas, section (fig. 12) the flight was forced higher and higher in order to clear an active instability line. Since the flight was made at an angle of only 20 degrees to the line, the 100-mi. section shown is equivalent to a normal section of only 34 mi.

The relative humidity profile is similar in shape to the isentropic bulge with values ranging from 58% just east of Abilene to supersaturated maxima of 121% near the crest of the isentropic bulge.

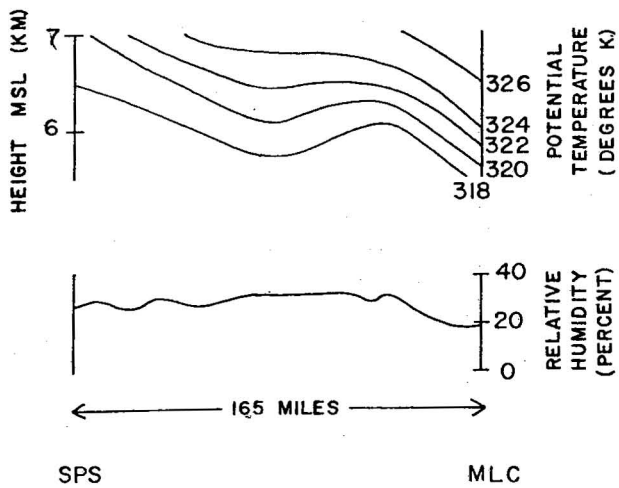

Figure 11.- Isentropic detail from a quasi-horizontal traverse through an incipient instability area between Wichita Falls, Texas, (SPS), and McAlester, Oklahoma (MLC), Flight 39, 1148-1330 CST, May 3, 1958.

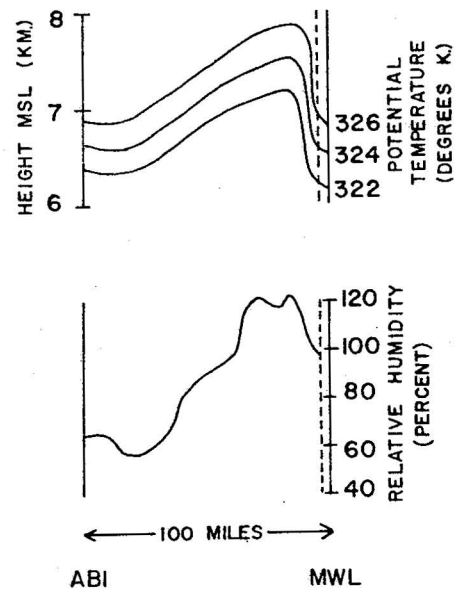

Figure 12.- Isentropic detail from a quasi-horizontal traverse through an active instability line between Abilene, Texas (ABI), and Mineral Wells, Texas (MWL), Flight 31, 1327-1422 CST, April 17, 1958.

Figure 13 shows the geometry of isentropes normal to an active instability line for the layer from 5.5 to 8.0 km. The section is a freehand composite based upon six cases. The cases were too varied and too few to permit actual averaging. Consequently the isentropes have not been given specific values, and their spacing is arbitrary. The section indicates that upward bulging of isentropes at higher levels may be considerable.

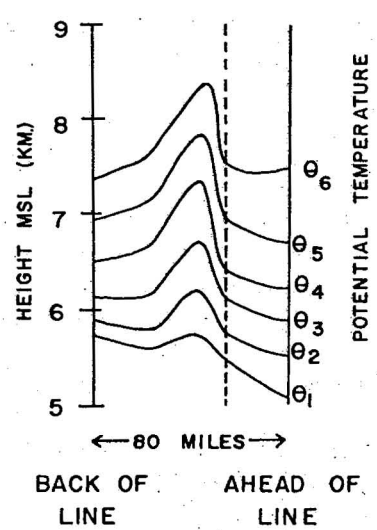

Figure 13.- Freehand composite of the isentropic detail through six active instability lines for the layer 5 to 8 km.

The upward bulging of isentropes in figures 9 - 13 indicate that the clear air in these portions of the instability lines was colder than the environments. In figures 10, 12, and 13 the slopes of the isentropic bulges are steeper on their leading edges than on their trailing edges, indicating greater gradients of temperature on the leading edges than on the trailing edges. In figure 12 it is indicated that the air is more nearly saturated in the isentropic bulge than it is in the environment.

8. ISENTROPIC GEOMETRY AND MOTION FIELDS

The isentropic features presented in the previous sections can be used to infer vertical motion fields. In this section these motion fields and their relationships to the instability line will be discussed. It will be shown that (1) the instability line environment is characterized by downslope motion through a considerable depth, (2) a zone of the instability line itself is characterized by upward motion, and (3) these motions resemble those occurring in the flow of water down an inclined channel under conditions of the hydraulic jump.

Motions with respect to isentropic surfaces. A flow can be assumed to follow isentropic surfaces if (1) the isentropic environment is quasistationary with respect to the flow through it, (2) condensation and evaporation do not occur, and (3) diabatic temperature changes are small. Upward motion results along positively tilted isentropes and downslope motion results along negatively tilted isentropes. When the environmental lapse rate of temperature is less than the dry adiabatic rate, upslope motion cools the parcel, while downslope motion warms it.

The above conditions were generally valid for the data used in this study. However, with respect to (1), the proper flow was definitely established in only one case. In this case (fig. 7) the west to east component of flow ranged from 11 to 24 m./sec. with respect to an incipient line which was reasoned to have been virtually stationary. In one other case (fig. 8) the flow was questionable. No other cases were examined. The conditions in (2) and (3) were met, since flights were made in clear air and at sufficient height to be above the effects of surface heating. The temperature lapse rates at the levels considered were all less than the dry adiabatic rate.

Downslope motion in the instability line environment. Assuming that components of horizontal flow existed from left to right in figures 5 and 6, there would have been downslope motion along the negatively tilted isentropes in the layers from about 2 to at least 5 km. That this downslope motion may be a universal feature of all instability line environments is indicated by the fact that individual cases were everywhere characterized by negatively tilted isentropes in the layer from 4 to 5 km. Although the layer of downslope motion was of greater depth for individual cases, it is suggested by the data that the layer from 4 to 5 km. is preferred. An idealized motion field of the instability line environment is shown in figure 14. The dashed line, *AB*, indicates the vertical plane of the instability line.

Upward motion in the instability line. Upward motion along the instability line is indicated by the upward bulging of isentropes, as shown in

figures 9 - 13. Further evidence of the upward motion is found in the greater relative humidity of the isentropic bulge with respect to the environment as shown in figures 11 and 12. This difference is very striking in figure 12, where the geometry of the relative humidity profile closely approximates that of the isentropic bulge.

Upward motion in the isentropic bulge should be considered as a net upward displacement with respect to the environment. Individual parcels would actually rise on the rear side of the bulge and descend on the leading side. The fact that the visual or radar width of the active instability line was sometimes less than the width of the isentropic bulge may have resulted from the fact that individual parcels on the leading side of the bulge were descending. This appears to have been the case in figure 9, where some of the isentropic bulge was present in advance of the leading edge of the active instability line.

A quantitative relationship between the vertical displacement of parcels in the isentropic bulge and the changes in relative humidity can be shown. In figure 12 the height of the 326° K. isentrope ranged from 6.9 km. at the minimum point of 58% relative humidity to 7.8 km. at the second maximum point of 121% relative humidity. By referring to a pseudo-adiabatic chart it is found that a 58% relative humidity at 6.9 km. and 326° K. corresponds to a mixing ratio of approximately 1.2 gm./kg. Lifting a parcel dry adiabatically from this point to 7.8 km. reduces its saturation mixing ratio to approximately 1.0 gm./kg. Its relative humidity would then be 1.2/1.0 or 120%, which is in excellent agreement with the observed value of 121%.

Data were checked to ascertain if the supersaturated values of relative humidity in figure 12 were correct. No errors were found and it is assumed that the supersaturated condition did exist. Insufficient data have been examined, however, to ascertain whether or not the condition is typical. It could result, especially at higher levels, as a consequence of insufficient condensation nuclei, and it might represent a lag between saturation and condensation in the case of rapidly building clouds. It is noteworthy in figure 12 that the flight was made above clouds and that it was forced higher and higher as the clouds continued to build.

An idealized motion field of the instability line with respect to its environment is shown in figure 15. The section *BACD* is the region of net upward displacement and represents the instability line in its pre-cloud stage. Although the same basic flow might be present within the cloud stage, internal flow patterns of the active thunderstorms would greatly modify and could even mask the basic flow.

Significance of the motion fields. The upward displacement of parcels in *BACD* of figure 15 may be considered as the immediate mechanism of the active instability line. Continued upward displacement of parcels in a conditionally unstable atmosphere would result in free convection and the formation of thunderstorms.

The downslope flow in figure 14 and 15 may be one of the elements in the overall mechanism of the instability line. Such flow is frequently observed down cold frontal surfaces and along lee slopes of mountain barriers. Instability lines show a preference for these areas.

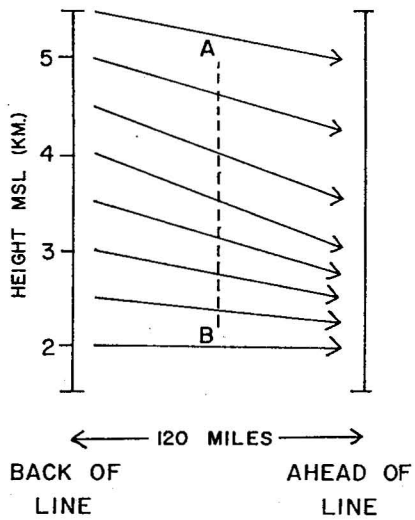

Figure 14.- Space cross section of the flow in the instability line environment.

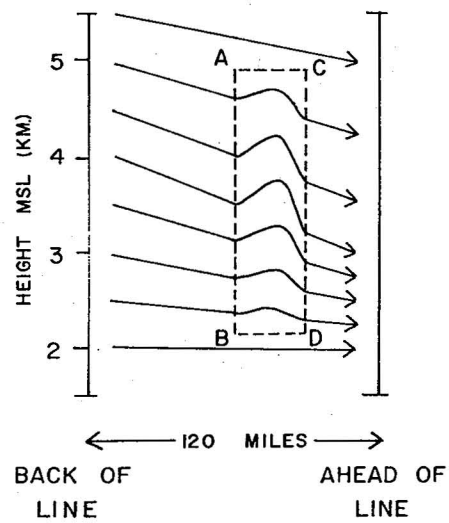

Figure 15.- Space cross section of the flow through the instability line and its environment.

The flow indicated in *BACD* of figure 15 is similar in appearance to the standing wave or hydraulic jump that can occur in the flow of water in an open channel. When certain critical values of depth and velocity of flow are reached, the horizontal flow is interrupted and translated upward as a hydraulic jump. When the channel is inclined, gravity may accelerate the flow so that a point will exist along the incline at which critical depth and velocity are reached. If an analogy is made between water flow and atmospheric flow, the line, *AB*, in figure 14 would indicate the portion of the channel in which critical depth and velocity would soon be reached. In figure 15 the section, *BACD*, would then be the region of an atmospheric jump.

Unfortunately the analogy is much too simple. Atmospheric flow is complicated by the compressibility of air, its stability, and its internal energy. These complexities have been realized by many authors, who have studied wave mechanisms in the atmosphere. Early work was accomplished by McGurrin [5] and Freeman [6]. Further work by Tepper [7] related atmospheric waves to pressure jumps. In spite of these and other studies, doubt still exists as to the proper role of atmospheric waves as mechanisms for instability lines. The data presented here do not eliminate the doubt, but they do suggest that more data of the sort, together with detailed winds aloft data, should be sought in an effort to better define flow patterns with respect to instability lines and their environments.

9. SUMMARY

The data used demonstrate the capabilities of instrumented aircraft in obtaining small scale measurements in the atmosphere. Not only were the soundings spaced more closely than those of conventional stations; they were also strategically located and timed with respect to the features of interest. In addition, the traverse data provided the only horizontal link between sounding data at levels above the ground.

Average soundings ahead of the instability line were more unstable than those behind the line, and instability was greater with respect to active lines than with respect to incipient lines.

Average low level moisture ahead of the instability line exceeded that behind the line in both the incipient and active stages. It was more stratified in the incipient stage than in the active stage. Average quantities of moisture in the active stage were greater level for level than in the incipient stage.

Except at low levels the average environment of incipient and active instability lines was featured by negatively tilted isentropes. The maximum negative slope was located slightly above 4 km. Negative slope was present, without exception, for every case in the layer from 4 to 5 km. Negative slope of isentropes was interpreted as downslope motion in the instability line environment.

The negative slope of isentropes was considerably greater in two severe instability line cases than it was for the average cases. It is indicated that the amount of isentropic slope may be related to the severity of storms.

Although embedded in an average environment of negatively tilted isentropes, the instability line itself was featured by an upward bulging of the isentropes. This upward bulge was interpreted as an upward displacement of parcels in the instability line.

Conditions of flow in the instability line and its environment were found to resemble those of the hydraulic jump.

The findings and ideas presented here should be considered tentative. More observations will be required to substantiate some of the findings and to provide additional detail. More traverse observations, made frequently at many levels, are required to better portray the isentropic and moisture fields and their rates of change within the instability line. Detailed wind observations are also required to determine fields of flow, which for the present have been assumed or determined qualitatively by indirect methods. Observations, restricted here to clear air portions of instability lines, should be extended to include cloud portions as well. Finally, theoretical work on models like the one mentioned in Section 8 should be continued.

REFERENCES

1. Williams, D. T., "The National Severe Local Storms Research Project," *Weatherwise*, vol. 13, No. 3, June 1960, pp. 99-100.

2. Lee, J. T., and C. L. David, "Squall Line Structure and Development as Depicted by Horizontal Traverses by the Tornado Research Aircraft," *Bulletin of the American Meteorological Society*, vol. 42, No. 9, Sept. 1961, pp. 595-602.

3. Showalter, A. K., "A Stability Index for Thunderstorm Forecasting," *Bulletin of the American Meteorological Society*, vol. 34, No. 6, June 1953, pp. 250-252.

4. Fulks, J. R., "The Instability Line," *Compendium of Meteorology*, American Meteorological Society, Boston, Mass., 1951, pp. 647-652.

5. McGurrin, M., "The Principles of Open Channel Flow Applied to the Formation of Tornadoes," 1942, (Unpublished. Manuscript available in U. S. Weather Bureau Library).

6. Freeman, J. C., Jr., "An Analogy Between the Equatorial Easterlies and Supersonic Gas Flows," *Journal of Meteorology*, vol. 5, No. 4, Aug. 1948, pp. 138-146.

7. Tepper, M., "The Application of the Hydraulic Analogy to Certain Atmospheric Flow Problems," U. S. Weather Bureau *Research Paper No. 35*, 1952, 50 pp.

USCOMM-WB-DC